Nanoscale

ARTICLE

Superhydrophilic Cement-Coated Mesh: An Acid, Alkali, and Organic Reagent-Free Material for Oil/Water Separation

Received 00th January 2017,
Accepted 00th January 2017

DOI: 10.1039/x0xx00000x

www.rsc.org/

Jinlong Song,[#ab] Shude Li,[#ab] Changlin Zhao,[ab] Yao Lu,[c] Danyang Zhao,[ab] Jing Sun,*[a] Tamal Roy[d], Claire J. Carmalt,[e] Xu Deng[f] and Ivan P. Parkin[e]

Extreme wettability materials applied in oil/water separation have become a research focus in modern society, owing to the large amount of oil-containing industrial wastewater emissions and the frequent occurrence of oil spills. However, most of the methods to fabricate the extreme wettability materials involve toxic chemical reagents, complex chemical reaction processes, and dangerous operation processes. A new acid, alkali, and organic reagent-free cement-coated mesh was presented for the sustained separation of oil and water from oil/water mixture. The meshes were fabricated by dipping porous Cu meshes in the cement paste. The micro/nanostructures and hydroxyl groups of the cement endowed the meshes superhydrophilic in air and superoleophobic under water. The separation efficiencies for oils with a wide range of kinematic viscosities (0.42-74.4cSt at 40 °C) were all above 94%. The superhydrophilic cement-coated meshes could separate oil/water mixture containing hot water, salt, and alkali for at least 30 cycles. The superoleophobicity of the cement-coated meshes were intact under seawater for at least 120 hours, showing good durability and stability. This green fabrication method is easy, cost-effective and environment-friendly.

Introduction

Oil spills resulting from oil exploration and oil-contaminated wastewater emission from the petrochemical industry pose great environmental risk.[1-9] For oil spills, the oil film on the surface of water can hinder rehydration, reduce the dissolved oxygen, and kill aquatic plants and sealifes. Contaminating oil in wastewater, used for irrigation, clogs the pores of the soil and prevents the penetration of air, which further prevents normal metabolism of microorganisms, thereby reducing the yield of crops. Finding an effective solution to the problem of oil pollution in water has always been an important research topic. Traditional countermeasures to oil spill accidents, including microbial degradation,[10] in-situ combustion,[11] oil containment boom isolation,[12] and oil skimmer collection,[13] generally have disadvantages such as high toxicity, low separation efficiency, low selectivity, and poor recyclability. An effective methodology to separate oil/water mixtures is urgently demanded environmentally as well as economically. In the past decades, the extreme wettability materials, including superhydrophobic-superoleophilic materials and superhydrophilic-underwater-superoleophobic materials, have attracted increasing attention for oil/water separation due to the distinct interfacial properties of oil and water.[14-37] The separation methods based on the extreme wettability of materials were classified into two categories: the absorption method and the filtration method.[38,39] Compared to absorption, the filtration method has gained more popularity because of its higher separation flux and higher separation efficiency. The extreme wettability filtration materials (EWFM) are often fabricated on porous metal mesh, textiles/fabrics, and polymeric membranes.[40-55] Although there are dozens of methods to fabricate the extreme wettability filtration materials, almost all of the methods involve toxic chemical reagents, complex chemical reactions, and dangerous operation processes. For example, Zhang et al. immersed a Cu mesh in an aqueous solution of NaOH and $(NH_4)_2S_2O_8$ to form the superhydrophilic $Cu(OH)_2$ nanowires coated mesh and enabling oil/water separation.[43] Song et al. immersed a stainless steel mesh in a mixture of $CuCl_2$ and HCl to deposit superhydrophilic leaf-like Cu structures on the surface of the mesh.[56] Yu and Raturi respectively used high temperature (1000 °C) heat treatment to grow superhydrophilic NiO particles on Ni mesh and ZnO nanowires on stainless steel mesh.[57,58] Yin et al. used femtosecond laser to etch the stainless steel to construct microstructures and

[a] Key Laboratory for Precision and Non-traditional Machining Technology of the Ministry of Education, Dalian University of Technology, Dalian 116024, P. R. China. Email: sunjing@dlut.edu.cn
[b] Collaborative Innovation Center of Major Machine Manufacturing in Liaoning, Dalian University of Technology, Dalian 116024, China.
[c] Nanoengineered Systems Laboratory, UCL Mechanical Engineering, University College London, London, WC1E 7JE, UK
[d] Institute for Nano-and-Microfluidics, Technische Universität Darmstadt, Darmstadt 64287, Germany
[e] Department of Chemistry, University College London, 20 Gordon Street, London, WC1H 0AJ, UK.
[f] Institute of Fundamental and Frontier Sciences, University of Electronic Science and Technology of China, Chengdu 610054, P. R. China.
[#] Contribute equally

† Electronic Supplementary Information (ESI) available: [details of any supplementary information available should be included here]. See DOI: 10.1039/x0xx00000x

superhydrophilicity.[59] Gu et al. immersed polylactic acid (PLA) nonwoven fabric into a tris-buffer solution of dopamine, SiO_2 nanoparticles and polystyrene microspheres to prepare superhydrophobic-superoleophilic SiO_2/PS/PLA nonwoven fabric.[60] Zhang et al. reported an inert solvent-induced phase-inversion process, which includes dissolving poly (vinylidene fluoride) (PVDF) in N-Methyl pyrrolidone solution followed by addition of ammonia water, to fabricate a superhydrophobic and superoleophilic PVDF membrane.[41] Fan et al. fabricated hydrogel-coated filter paper for oil/water separation by smartly crosslinking filter paper with hydrophilic polyvinyl alcohol through a simple alcohol condensation reaction with glutaraldehyde as a crosslinker.[61] Liu et al. fabricated various translucent superhydrophobic filtration materials by spraying the hybrids of PDMS, PMMA, and tetrahydrofuran mixtures on different substrates.[62] Some other porous polymer membrane were also synthesised to separate oil/water mixture.[63, 64] Environment-friendly, cost-effective, and easy fabrication of the extreme wettability filtration materials is the pursuit of many researchers and will promote the practical application of the extreme wettability filtration materials.

Cement, the main composition of concrete, is widely used in individual, commercial and public architecture. Here, we simply mixed cement and water to form a superhydrophilic paste and treated the paste onto copper mesh without using any acidic, alkaline and organic reagents and complex reactions. The meshes showed superhydrophilicity in air and superoleophobicity under water and had high separation efficiencies of oils with different kinematic viscosities above 94%. The cement-coated mesh also showed high reusability and stability through repeated oil/water separation tests with alkali, salt, and boiling water, and retained its high separation efficiency even after 120 hours storage in seawater. This easy, low-cost and environmentally-friendly method has great potential to be applied for large scale industrial oil/water separation and cleaning-up oil spills on the contaminated water.

Experiment Section

Materials

Ordinary Portland cement (PO 42.5) was purchased from Guangdong Tapai Co., Ltd. (China). Copper (Cu) meshes with pore size of 450 μm and wire size of 45 μm were purchased from Shanghai Hengxin Wire Mesh Co., Ltd. (China). Hexane and dichloromethane were purchased from Sigma-Aldrich (USA). Diesel and lubricating oil were purchased from China National Petroleum Corporation. Peanut oil was purchased from Luhua Co. (China).

Preparation of superhydrophilic cement-coated meshes

Copper meshes were first cut into circular pieces with diameter of 50 mm and then washed in detergent, anhydrous ethanol and water. Cement and water with different mass ratios were put into a beaker and stirred uniformly to form a fresh hydraulic cement paste. Then, the Cu meshes were immersed in the cement paste for about 30 s and pulled out at a velocity of 0.01 m/s. After curing into a rigid mass at room temperature for 5 h, the superhydrophilic cement-coated meshes were obtained. The relationship between the cement mass per unit area of the obtained cement-coated meshes with the mass ratio of water and cement in the fresh hydraulic cement paste was shown in Fig. 1.

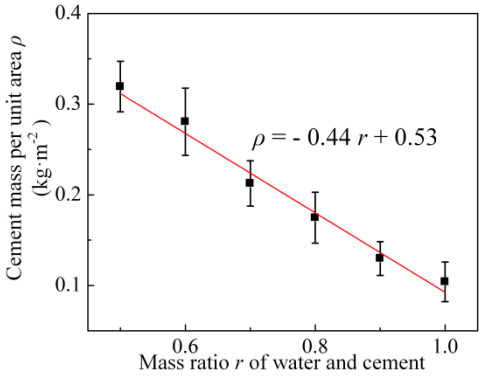

Fig.1 The variation of the cement mass per unit area ρ of the obtained cement-coated meshes with the mass ratio r of water and cement in the fresh hydraulic cement paste.

Oil/water separation

Before the oil/water separation, the superhydrophilic cement-coated meshes were immersed in water for 1 min to make it suffused with water and repellent to oil. Only in this condition, the water will pass through the meshes with the oil retained above the meshes. The superhydrophilic cement-coated meshes were fixed between two transparent acrylic tubes of similar inner diameter of 36 mm with clamping devices. Then, the oil/water mixture was poured onto the upper tube and separated. The separated oil was collected for evaluating the separation efficiency. The basic parameters of oil used in the oil/water separation experiments are shown in Table 1.

Characterization

Contact angles (CAs) and sliding angles (SAs) of water and oil were measured by an optical contact angle measurement device (Krüss, DSA100, Germany) using ~5 μL water and oil droplets at room temperature. Surface morphologies of the superhydrophilic cement-coated meshes were observed by a field emission scanning electron microscope (SEM, JSM-6360LV, Japan), and the corresponding chemical composition of the surface was characterized by an X-ray diffractometer (XRD-6000, Japan). The separated oil was characterized by Fourier transform infrared spectrum (FTIR, ThermoFisher 6700, USA) to verify whether the oil contained water. Additionally, the oil content in the collected water was determined from the absorbance peak intensity of FTIR. The residual oil was extracted by CCl_4 from the permeated water, and then the absorbance intensity values 2857, 2925, and 2958 cm^{-1} were used to determine the oil content. The separation efficiency, R, of oil/water mixture was calculated by the ratio between the collected oil mass M_c and the oil mass of the original oil/water mixture M_o (R (%) = (M_c / M_o) × 100%). The water mass flux

(F_{water}) in the oil/water separation was calculated by $F_{water} = V /$ is the cross sectional area of the mesh that was exposed to oil/water mixture, and t is the required time for the complete permeation of water. The cement mass per unit area ΔM on the meshes was calculated by $\Delta M = (M_b - M_a) / S$, where M_a and M_b are the mass of the meshes before and after cement coating. The oils used in the present study include hexane, diesel, peanut oil, lubricating oil, and dichloromethane. The relevant properties of different types of oil are summarized in Table 1.

Results and discussion

Fig. 2 shows the surface morphology and chemical composition of the ordinary copper meshes and the superhydrophilic cement-coated Cu meshes. For the ordinary Cu meshes, the wire surfaces were very smooth, as shown in ($S \cdot t$), where V is the water volume in the oil/water mixtures, S Figs. 2a to 2c. The average size of the wire diameter and open pores were 45 μm and 450 μm, respectively. After immersing in the cement paste, the pores were clogged by the rigid mass of the cement, as shown in Fig. 2d. The magnified SEM images show that the cement rigid mass was not smooth but composed of micrometer-scale lump-like structures with size of 10 μm-40 μm, micrometer-scale and submicrometer-scale pores with size of 100 nm-20 μm, and nanometer-scale wires with diameter of about 25 nm. All nanowires grew vertical to the substrate, as shown in Figs. 2e and 2f. The XRD pattern indicates that the main composition of the cement rigid mass was calcium silicate hydrate, calcium hydroxide and ettringite, which contains a large number of hydroxyl groups, as shown in Fig. 2g. The hydroxyl groups and micro/nano structures enable the cement-coated mesh to be superhydrophilic.

Table 1 Properties of oils used in the experiments

Oil	Hexane	Diesel	Peanut oil	Lubricating oil	Dichloromethane
Density at 25°C[g/cm^3]	0.65	0.84	0.92	0.84	1.325
Surface tension at 20°C [mN/m]	17.9	28.3	34.5	40.1	21.3
Kinematic viscosity at 40°C [cSt]	0.42	4.33	39.6	74.4	0.33

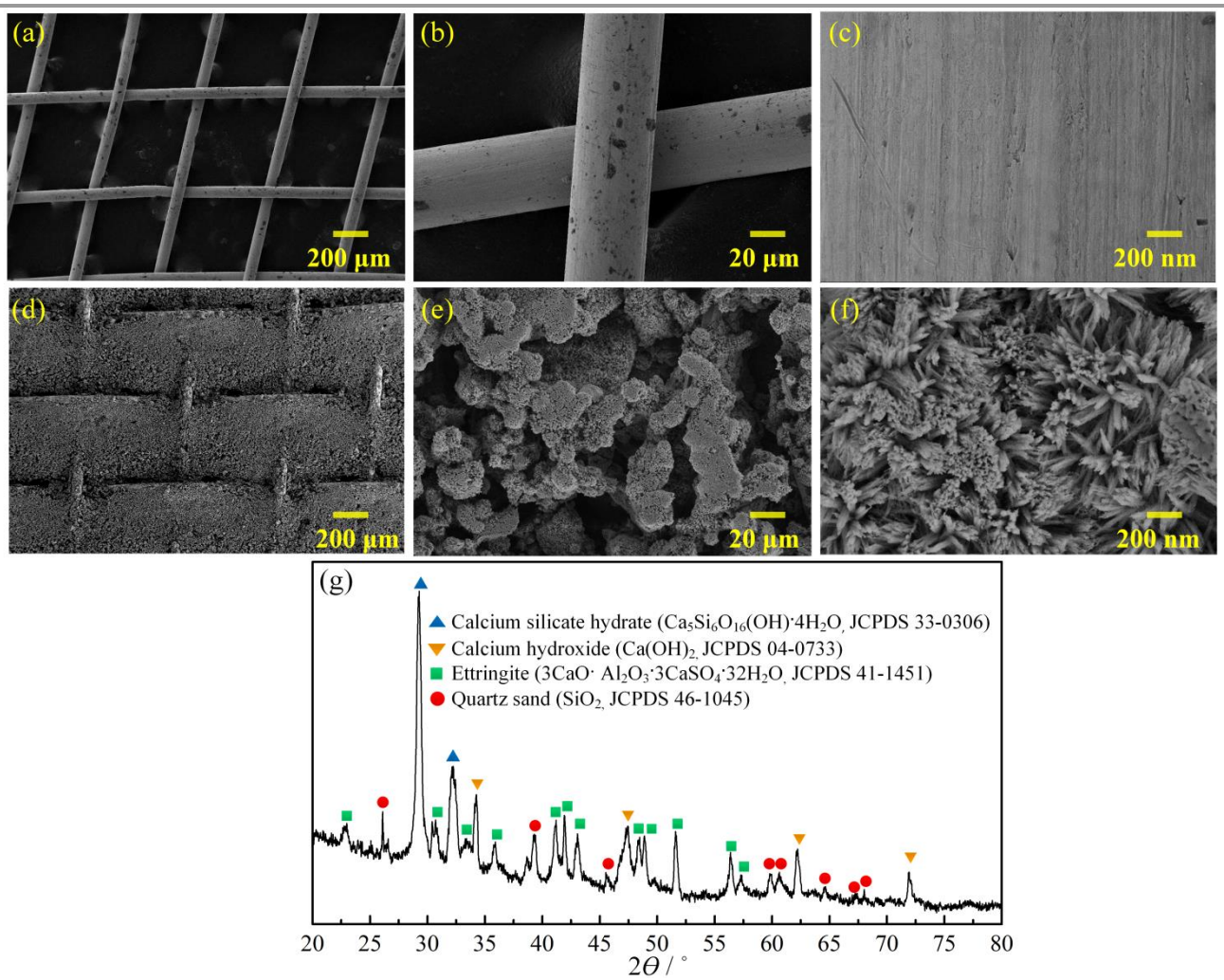

Fig. 2 Surface morphology and chemical composition of the superhydrophilic cement-coated meshes: (a)-(c) SEM images of the ordinary Cu meshes, (d)-(f) SEM images of the cement-coated Cu mesh with 0.17 kg/m^2 cement mass per unit area, and (g) XRD pattern of the cement-coated Cu meshes.

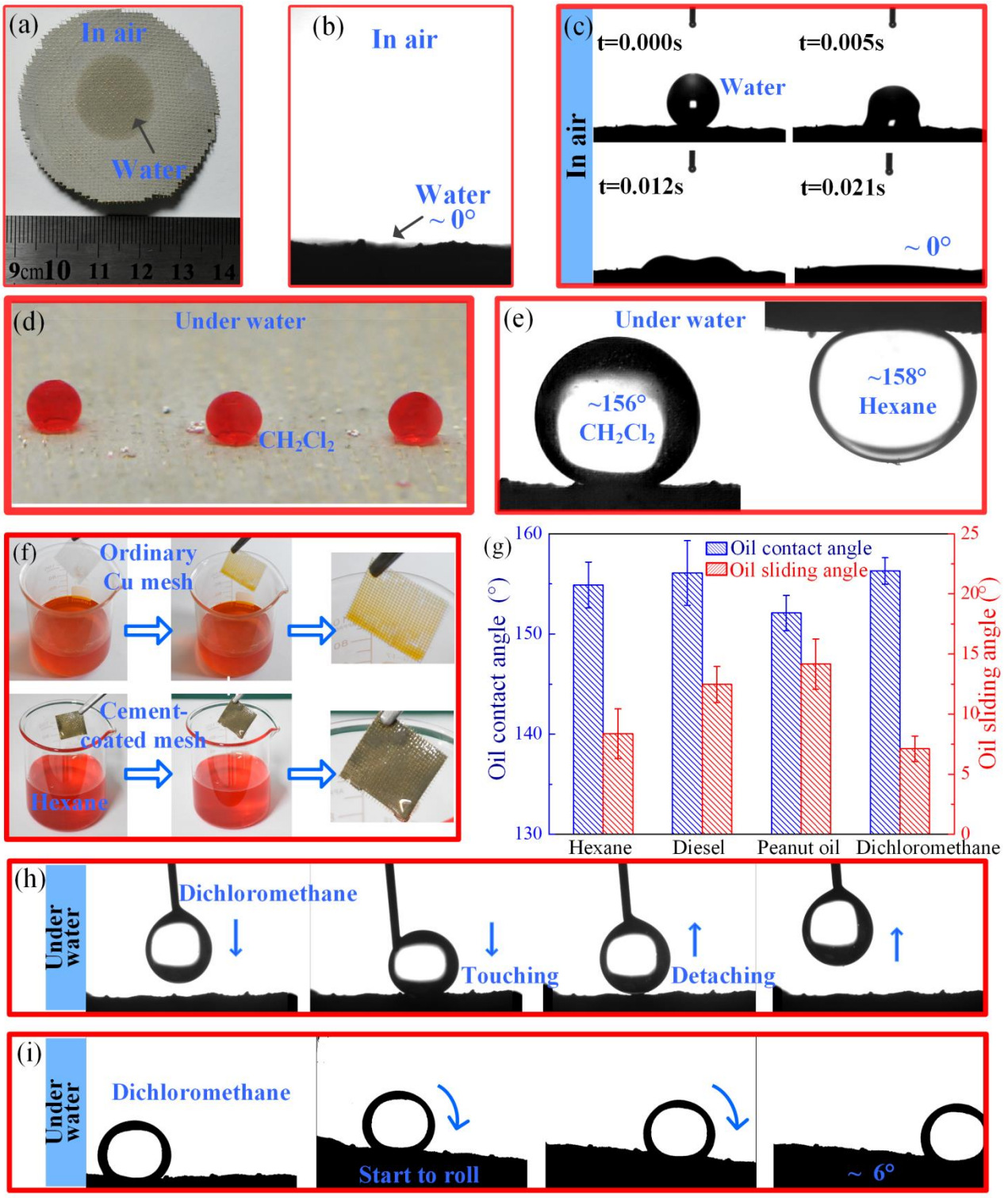

Fig. 3 Superhydrophilic and underwater superoleophobic properties of the cement-coated meshes with 0.17 kg/m² cement mass per unit area: (a)-(c) photograph of water droplet on the cement-coated meshes in air, (d)-(e) photograph of 5 μL oil droplets on the cement-coated meshes under water, (f) photos of the ordinary Cu meshes and the water pre-suffused cement-coated meshes immersed in hexane, (g) the underwater contact angles and sliding angles of hexane, diesel, peanut oil and dichloromethane on the cement-coated meshes, and (h)-(i) the contacting, detachment, and rolling off processes of oil droplets on the underwater superoleophobic cement-coated meshes.

Figs. 3a to 3c show the superhydrophilicity of the cement-coated meshes. The water droplet spread rapidly and completely within 0.021 s on the meshes with water contact angle of about 0°. When the superhydrophilic cement-coated meshes were immersed in water, the water penetrated and became entrapped in the rough micro/nano-scale structures, forming a repellent conformal barrier to oil droplets and showing underwater superoleophobicity.[65] Oil droplets on the underwater cement-coated meshes form a spherical shape, as shown in Figs. 3d and 3e. Fig. 3f shows that the cement-coated

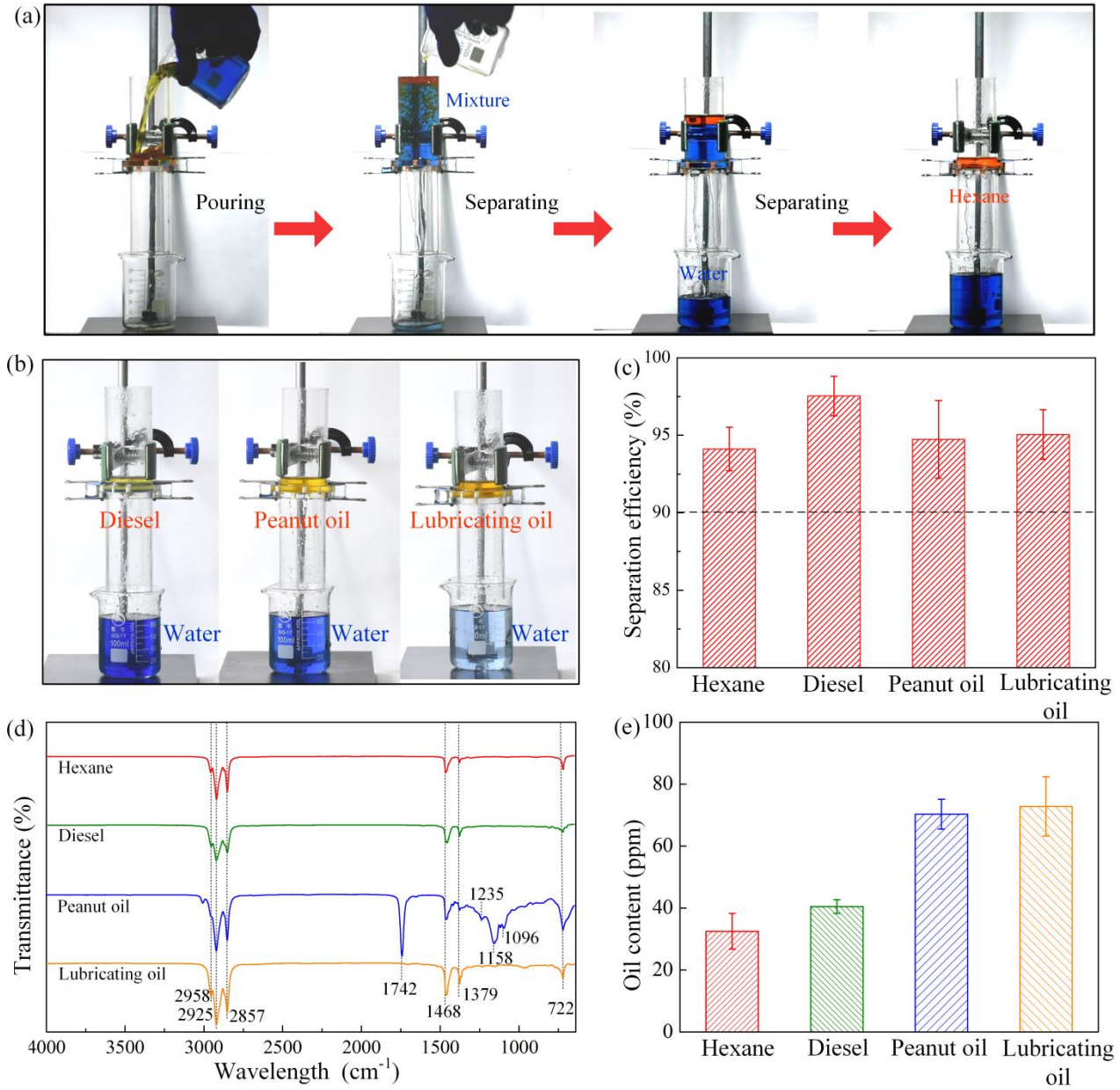

Fig. 4 Separation of oil/water mixtures by the cement-coated meshes with 0.17 kg/m² cement mass per unit area: (a) and (b) depicts the separation processes of hexane/water mixture, diesel oil/water mixture, peanut oil/water mixture and lubricating oil/water mixture, (c) the separation efficiency of the superhydrophilic cement-coated meshes for different types of the oil, (d) the FTIR spectra of the separated oils, and (e) the oil content in the collected water.

meshes, pre-suffused with water, had superior oil repellence while the ordinary copper meshes were easily contaminated by oil. Fig. 3g shows the underwater contact angles and sliding angles of oil droplets with different kinematic viscosities on the superhydrophilic cement-coated meshes. The contact angles of hexane, diesel, peanut oil and dichloromethane, were 155°, 156°, 152°, and 156°, respectively. The sliding angles of the aforementioned four oils were 8°, 12°, 14°, and 7°, respectively, indicating the ultralow underwater adhesion to oils. Figs. 3h, 3i and Video S1 and S2 show the contacting, detachment, and rolling off processes of oil droplets on the underwater superoleophobic cement-coated meshes. The oil droplets in contact showed an easy detachment from the meshes.

Due to their excellent superhydrophilicity in air and superoleophobicity under water, the cement-coated meshes were used to separate oil/water mixtures. Figs. 4a, 4b and Video S3 show the separation processes of oil/water mixture driven by gravity. Hexane, diesel, peanut oil, and lubricating oil with different kinematic viscosities were used as the floating oil. Oil/water mixtures were poured onto the as-prepared cement-coated meshes mounted between two acrylic tubes. No external force, except gravity, acted during the ensuing separation process. Before separation, the superhydrophilic cement-coated meshes were pre-suffused with water. Although the lighter oil phase encountered the mesh first and spread rapidly and completely during pouring, it could not pass through the mesh, due to the presence of the trapped water in oil which was retained above the mesh, enabling the oil/water mixture to be completely separated. The separation efficiency of the superhydrophilic cement-coated meshes was all above 94% and even reached up to 98% for diesel oil/water mixture,

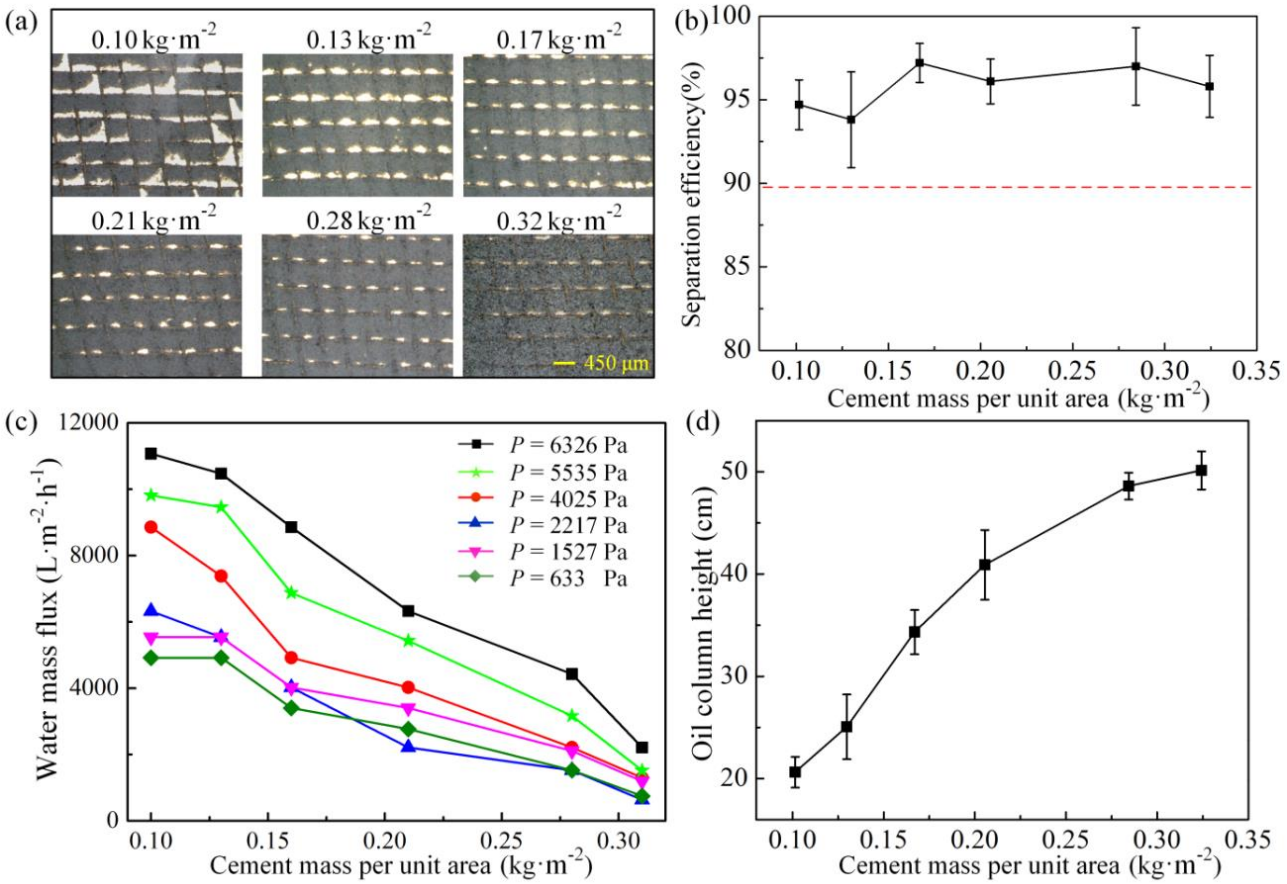

Fig. 5 The influence of the cement mass per unit area in separating hexane/water mixture: (a) the microscopy images of the cement-coated meshes with different cement mass per unit area, (b) the variation of the separation efficiency with the cement mass per unit area, (c) the variation of the water mass flux with the cement mass per unit area, and (d) the variation of the liquid column height with the cement mass per unit area.

as shown in Fig. 4c. The purity of the separated oil and water is another important parameter to characterize the separation performance of the cement-coated meshes. The purity of the separated oil and water were investigated by Fourier-transform infrared spectrophotometer (FTIR). Fig. 4d shows the FTIR spectra of the collected oils, all the absorption bands corresponded to the characteristic vibrations of alkanes (the chemical constituents of hexane, diesel, peanut oil and lubricating oil) and ester groups (the chemical constituents of peanut oil). The bands from 2857 to 2958 cm^{-1} were assigned to the -C-H asymmetric and symmetric stretching vibration of the $-CH_3-$ and $-CH_2-$ groups. The band at 1742 cm^{-1} corresponded to the -C=O stretching vibration of ester groups. The bands at 1468 and 1379 cm^{-1} were both assigned to the -CH asymmetric and symmetric bending vibration of the $-CH_3-$ groups. The bands from 1158 to 1235 cm^{-1} were attributed to the -C-H wagging vibration of $-CH_2-$ groups. The band at 1096 cm^{-1} was assigned to -C-O stretching vibration of ester groups. The band at 722 cm^{-1} was corresponding to -C-H rocking vibration of $-CH_2-$ groups. No band assigned to water was observed, confirming the high purity of the collected oil. Additionally, the oil content in the collected water was determined and is depicted in Fig. 4e. All oils present in the collected water were lower than 80 ppm, and in particular, hexane in water was lower than 35 ppm, indicating the high purity of the collected water.

We also measured the water mass flux in the oil/water separation processes. It is well known that the flux is dependent on the pressure of liquid and pore size of the meshes. Here, we realized the control of the flux under a certain pressure by adjusting the cement mass per unit area on the meshes. Fig. 5a shows the microscopy images of the cement-coated meshes with different cement mass per unit area. Although, the different cement mass per unit area does not affect the micro/nanometer-scale structures, as shown in Fig. S1, the pore size on the meshes decreased with the increased cement mass per unit area. Although the influence of the cement mass per unit area on separation efficiency was negligible (Fig. 5b), the water mass flux varied significantly. Fig. 5c shows the variation of the mass flux of water in the separation processes under different values of pressure with the cement mass per unit area. The flux decreased with an increase in the cement mass per unit area which can be attributed to the decreased pore size. The largest flux was obtained at the cement mass per unit area of 0.1 kg/m^2. We also measured the variation of the maximum height of the oil column that the mesh could support without penetrating through the cement mass. The oil column height increased with the increase of the cement mass per unit area, as shown in Fig. 5d. The maximum height of the liquid column of 50 cm was obtained at the cement mass per unit area of 0.32 kg/m^2. Since the superhydrophilic cement-coated meshes still show

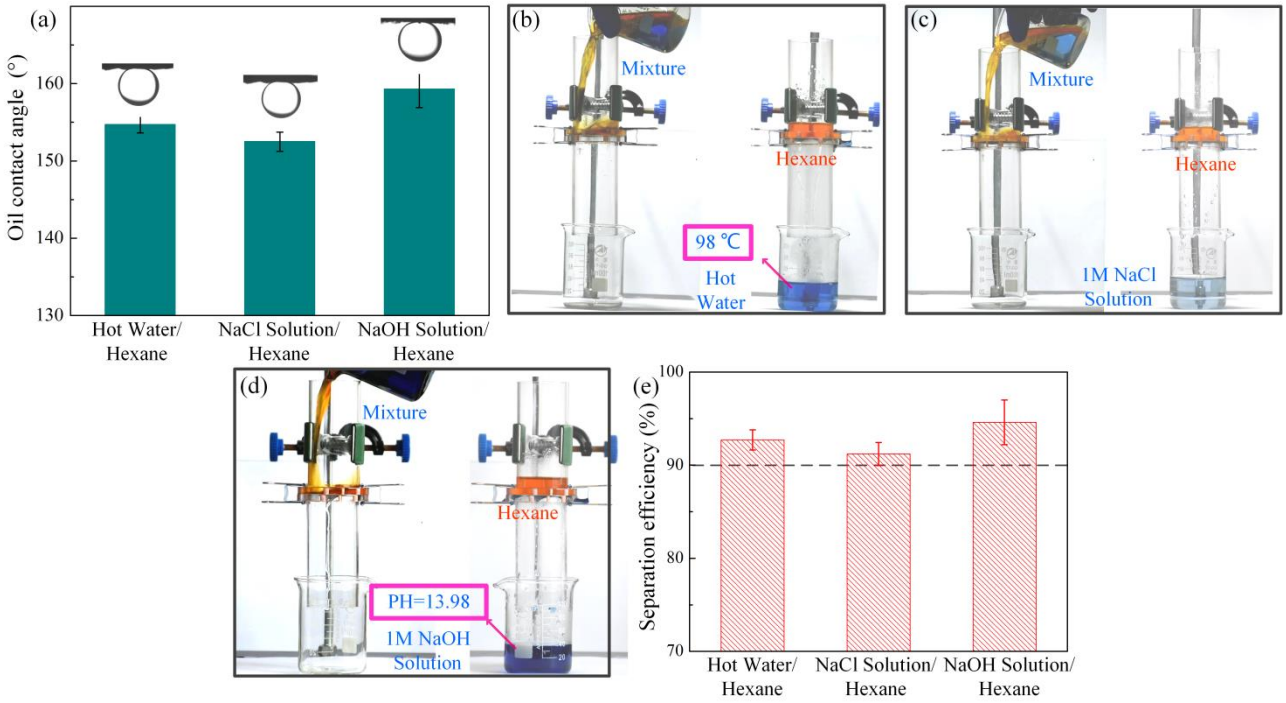

Fig. 6 Separation of oil/water mixtures containing hot water, salt, and alkali (the cement mass per unit area of the meshes is 0.17 kg/m²): (a) CAs of hexane on the superhydrophilic cement-coated meshes under hot water, salt water, and alkaline water, (b) the separation process of hexane/hot water mixture, (c) the separation process of hexane/NaCl solution mixture, (d) the separation process of hexane/NaOH solution mixture, (e) the separation efficiencies of hexane/hot water mixture, hexane/NaCl solution mixture, and hexane/NaOH solution mixture.

superoleophobicity under hot water, salt water, and alkaline water with CAs above 150° (Fig. 6a and Fig. S2(a)), we successfully realized the separation of water and oil from oil/water mixtures containing hot water (98 °C), salt, or alkali. Figs. 6b to 6d and Fig. S2(b) show the separation processes of hexane/hot water mixture, hexane/NaCl solution mixture, hexane/NaOH solution mixture, hexane/$MgCl_2$ solution mixture, hexane/Na_2CO_3 solution mixture, and hexane/Na_2SO_4 solution mixture, respectively. The water quickly passed through the meshes while the oils were retained above the meshes, realizing the complete separation of oil/water mixture with the separation efficiency larger than 90%, as shown in Fig. 6e and Fig. S2.

The superhydrophilic cement-coated meshes not only have good oil/water separation efficiency, but also have very respectable durability. Fig. 7(a) and Fig. S3 shows the variation of the water mass flux and separation efficiency with the hexane/seawater separation cycles and hexane/NaOH solution separation cycles. The water mass flux and separation efficiency kept stable at least for 30 cycles. We also characterized the underwater CAs and surface micro morphology of the cement-coated meshes after 30 cycles of oil/water separation, as shown in Figs. 7(b) and 7(c). The underwater CAs of hexane, diesel, peanut oil, and dichloromethane on the cement-coated meshes were still above 150° and the surface micro-morphology was almost same as before. We also tested the storage stability of the superhydrophilic cement-coated meshes under seawater, as shown in Fig. 7(d). After being placed under seawater for 120 hours, the cement-coated meshes still showed great superoleophobicity with CA of ~156°. In addition, Fig. 7(e) shows the processes of bending the superhydrophilic cement-coated mesh for 5 times. There is no damage for the mesh. All these results indicate that the superhydrophilic cement-coated meshes have good durability.

Conclusions

A new acid, alkali, and organic reagent-free cement-coated mesh was developed to separate oil/water mixtures in this work. Due to the micro/nanostructures and hydroxyl groups on the cement surfaces, the cement-coated meshes showed superhydrophilicity with a water contact angle of 0° in air and underwater superoleophobicity with oil contact angles >150°. The superhydrophilic cement-coated meshes achieve excellent oil/water separation efficiency (>94%) and high separation purities for oils with wide-ranging kinematic viscosities (0.42-74.4 cSt at 40°C), including lubricating oil. The durability and stability of the superhydrophilic cement-coated meshes were also good. The meshes not only could separate oil/water mixtures containing hot water, salt, and alkali but also could be effectively used after at least 30 cycles of separation or being stored in seawater for 120 hours. Moreover, the water separation mass flux was controlled by adjusting the cement mass per unit area. This environmental-friendly, low-cost, and easy method has the potential to be used in the treatment of oil spills and industrial wastewater.

Conflicts of interest

There are no conflicts to declare.

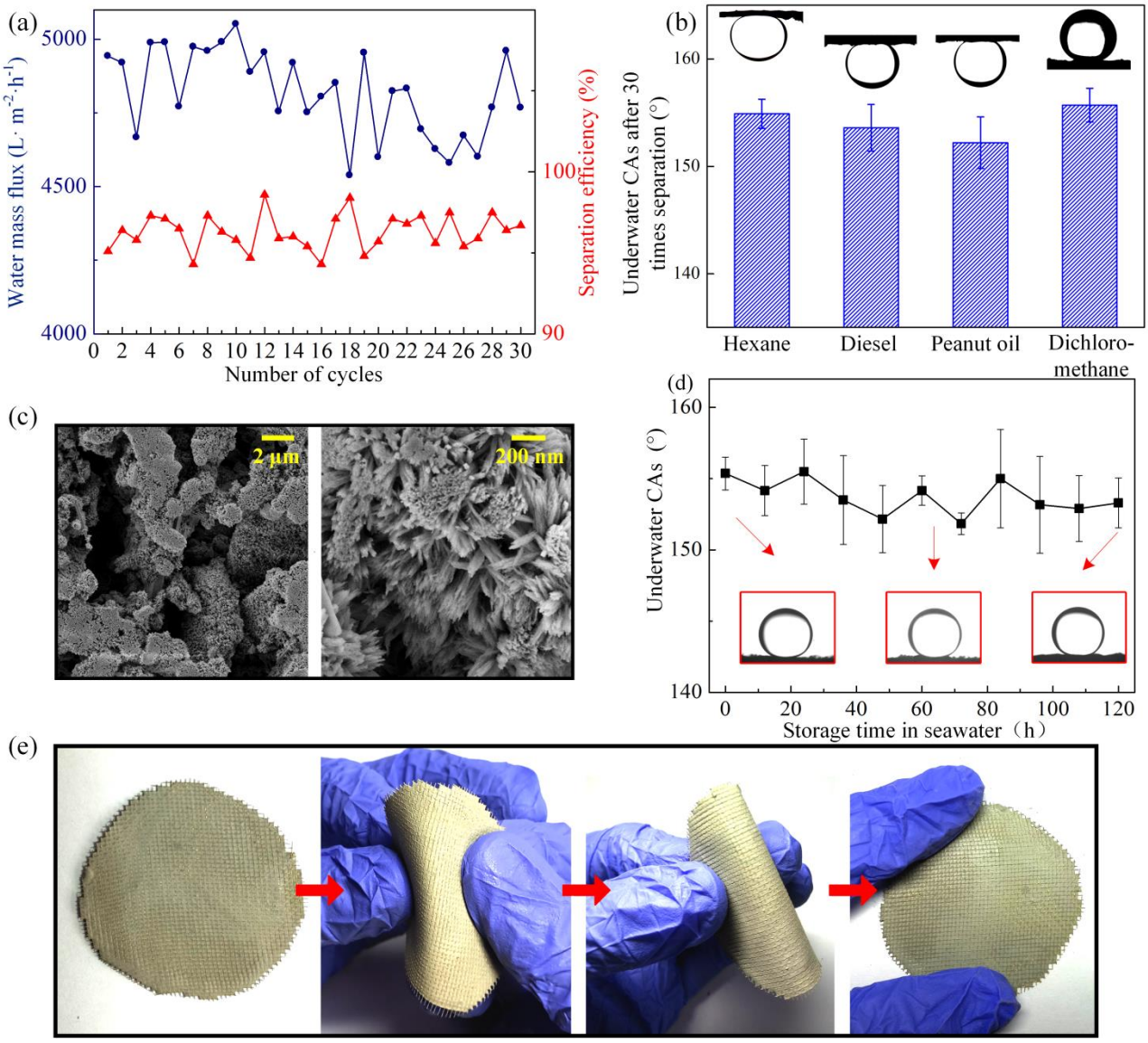

Fig. 7 The durability of the cement-coated meshes with 0.17 kg/m² cement mass per unit area: (a) the variation of the water mass flux and separation efficiency with the hexane/seawater separation cycles, (b) the underwater CAs of hexane, diesel oil, peanut oil and dichloromethane on the cement-coated meshes after 30 cycles of hexane/seawater separation, (c) SEM images of the superhydrophilic cement-coated meshes after 30 cycles of hexane/seawater separation, (d) the variation of the underwater CAs of dichloromethane on the superhydrophilic cement-coated meshes with the storage time in seawater, and (e) the processes of bending the superhydrophilic cement-coated mesh.

Acknowledgements

This project was financially supported by National Natural Science Foundation of China (NSFC, 51605078), Science Fund for Creative Research Groups of NSFC (51621064), National Basic Research Program of China (2015CB057304), and the Fundamental Research Funds for the Central Universities (DUT17JC25). Y. Lu acknowledges the support from EPSRC project EP/N024915/1.

Notes and references

1 J. Ge, L. Shi, Y. Wang, H. Zhao, H. Yao, Y. Zhu, Y. Zhang, H. Zhu, H. Wu and S. Yu, *Nat. Nanotechnol.*, 2017, 12, 434.
2 K. Jayaramulu, F. Geyer, M. Petr, R. Zboril, D. Vollmer and R. A. Fischer, *Adv. Mater.*, 2017, 29, 1605307.
3 K. Li, J. Ju, Z. Xue, J. Ma, L. Feng, S. Gao and L. Jiang, *Nat. Commun.*, 2013, 4.
4 Z. Chu, Y. Feng and S. Seeger, *Angew. Chem. Int. Edit.*, 2015, 54, 2328.
5 B. Wang, W. Liang, Z. Guo and W. Liu, Chem. *Soc. Rev.*, 2015, 44, 336.
6 Z. Xue, Y. Cao, N. Liu, L. Feng and L. Jiang, *J. Mater. Chem. A*, 2014, 2, 2445.
7 X. Gao, J. Zhou, R. Du, Z. Xie, S. Deng, R. Liu, Z. Liu and J. Zhang, *Adv. Mater.*, 2016, 28, 168.
8 S. Lee, B. Kim, S. Kim, E. Kim and J. Jang, *Adv. Funct. Mater.*, 2017, 02, 310.
9 T. Li, L. Wang, K. Zhang, Y. Xu, X. Long, S. Gao, R. Li and Y. Yao, *Small*, 2016, 12, 4960.
10 A. Bayat, S. F. Aghamiri, A. Moheb and G. R. Vakili-Nezhaad, *Chem. Eng. Technol.*, 2005, 28, 1525.
11 F. Chen, J. Song, Z. Liu, J. Liu, H. Zheng, S. Huang, J. Sun, W. Xu and X. Liu, *ACS Sustainable. Chem. Eng.*, 2016, 4, 6828.
12 S. P. Zhu and D. Strunin, *Spill Sci. Technol. Bull.*, 2002, 7, 249.

13 F. Chen, J. Liu, Y. Cui, S. Huang, J. Song, J. Sun, W. Xu and X. Liu, *J. Colloid* Interf. *Sci.*, 2016, 470, 221.
14 A. Turco, C. Malitesta, G. Barillaro, A. Greco, A. Maffezzoli and E. Mazzotta, *J. Mater. Chem. A,* 2015, 3, 17685.
15 N. Chen, Q. Pan and *ACS* Nano, 2013, 7, 6875.
16 Q. Zhu, Y. Chu, Z. Wang, N. Chen, L. Lin, F. Liu and Q. Pan, *J. Mater. Chem. A*, 2013, 1, 5386.
17 S. Nagappan, J. J. Park, S. S. Park, W. Lee and C. Ha, *J. Mater. Chem. A*, 2013, 1, 6761.
18 Q. Zhu, Q. Pan and F. Liu, *The Journal of Physical Chemistry C*, 2011, 115, 17464.
19 A. Sarkar and S. Mahapatra, *J. Mater. Chem. A*, 2014, 2, 3808.
20 P. Calcagnile, D. Fragouli, I. S. Bayer, G. C. Anyfantis, L. Martiradonna, P. D. Cozzoli, R. Cingolani and A. Athanassiou, *ACS Nano*, 2012, 6, 5413.
21 Q. Zhu and Q. Pan, *ACS Nano*, 2014, 8, 1402.
22 B. Wang, J. Li, G. Wang, W. Liang, Y. Zhang, L. Shi, Z. Guo and W. Liu, *ACS Appl. Mater. Inter.*, 2013, 5, 1827.
23 N. Cao, B. Yang, A. Barras, S. Szunerits and R. Boukherroub, *Chem. Eng. J.,* 2017, 307, 319.
24 J. Li, C. Xu, Y. Zhang, R. Wang, F. Zha and H. She, *J. Mater. Chem. A*, 2016, 4, 15546.
25 H. Zhu, S. Yang, D. Chen, N. Li, Q. Xu, H. Li, J. He and J. Lu, *Adv. Mater. Interfaces,* 2016, 3, 1500683.
26 L. Wu, L. Li, B. Li, J. Zhang and A. Wang, *ACS Appl. Mater, inter.*, 2015, 7, 4936.
27 C. Ruan, M. Shen, X. Ren, K. Ai and L. Lu, *Sci. Rep.-UK*, 2016, 6, 31233.
28 G. Hayase, K. Kanamori, M. Fukuchi, H. Kaji and K. Nakanishi, *Angew. Chem., Int. Ed*., 2013, 52, 1986.
29 S. Zhou, P. Liu, M. Wang, H. Zhao, J. Yang and F. Xu, *ACS Sustain. Chem. Eng.,* 2016, 4, 6409.
30 S. Wang, X. Peng, L. Zhong, J. Tan, S. Jing, X. Cao, W. Chen, C. Liu and R. Sun, *J. Mater. Chem. A*, 2015, 3, 8772.
31 Y. Tang, K. L. Yeo, Y. Chen, L. W. Yap, W. Xiong and W. Cheng, *J. Mater. Chem. A*, 2013, 1, 6723.
32 X. Gui, Z. Zeng, Z. Lin, Q. Gan, R. Xiang, Y. Zhu, A. Cao and Z. Tang, *ACS Appl. Mater. Inter*., 2013, 5, 5845.
33 X. Dong, J. Chen, Y. Ma, J. Wang, M. B. Chan-Park, X. Liu, L. Wang, W. Huang and P. Chen, *Chem. Commun*., 2012, 48, 10660.
34 L. Zhang, H. Li, X. Lai, X. Su, T. Liang and X. Zeng, *Chem*. *Eng. J*., 2017, 316, 736.
35 O. Oribayo, X. Feng, G. L. Rempel and Q. Pan, *Chem. Eng. J*., 2017, 323, 191.
36 A. R. Siddiqui, R. Maurya and K. Balani, *J. Mater. Chem. A*, 2017, 5, 2936.
37 Y. Yang, Z. Liu, J. Huang and C. Wang, *J. Mater. Chem. A*, 2015, 3, 5875.
38 H. Wang, E. Wang, Z. Liu, D. Gao, R. Yuan, L. Sun and Y. Zhu, *J. Mater. Chem. A*, 2015, 3, 266.
39 M. Tao, L. Xue, F. Liu, L. Jiang and *Adv. Mater*., 2014, 16, 2943.
40 Z. Shi, W. Zhang, F. Zhang, X. Liu, D. Wang, J. Jin and L. Jiang, *Adv. Mater*., 2013, 25, 2422.
41 W. Zhang, Z. Shi, F. Zhang, X. Liu, J. Jin and L. Jiang, *Adv. Mater*., 2013, 25, 2071.
42 W. Zhang, Y. Zhu, X. Liu, D. Wang, J. Li, L. Jiang and J. Jin, *Angew. Chem., Int. Ed*., 2014, 53, 856.
43 F. Zhang, W. B. Zhang, Z. Shi, D. Wang, J. Jin and L. Jiang, *Adv. Mater*., 2013, 25, 4192.
44 X. Zhou, Z. Zhang, X. Xu, F. Guo, X. Zhu, X. Men and B. Ge, *ACS Appl. Mater. Inter*., 2013, 5, 7208.
45 J. Gu, P. Xiao, P. Chen, L. Zhang, H. Wang, L. Dai, L. Song, Y. Huang, J. Zhang and T. Chen, *ACS Appl. Mater. Inter*., 2017, 9, 5968.
46 C. Cao, M. Ge, J. Huang, S. Li, S. Deng, S. Zhang, Z. Chen, K. Zhang, S. S. Al-Deyab and Y. Lai, *J. Mater. Chem. A*, 2016, 4, 12179.
47 Z. Xu, Y. Zhao, H. Wang, X. Wang and T. Lin, *Angew. Chem. Int. Edit.,* 2015, 54, 4.
48 X. Zheng, Z. Guo, D. Tian, X. Zhang, W. Li and L. Jiang, *ACS A Mater. Inter*., 2015, 7, 4336.
49 X. Zheng, Z. Guo, D. Tian, X. Zhang, W. Li and L. Jiang, *ACS Appl. Mater. Inter*., 2015, 7, 4336.
50 Y. Liu, X. Wang, B. Fei, H. Hu, C. Lai, J. H. Xin and *Adv. Funct. Mater.*, 2015, 25, 5047.
51 J. Y. Huang, S. H. Li, M. Z. Ge, L. N. Wang, T. L. Xing, G. Q. Chen, X. F. Liu, S. S. Al-Deyab, K. Q. Zhang, T. Chen and Y. K. Lai, *J. Mater. Chem. A*, 2015, 3, 2825.
52 A. K. Kota, G. Kwon, W. Choi, J. M. Mabry and A. Tuteja, *Nat. Commun.*, 2012, 3, 1025.
53 G. Kwon, A. K. Kota, Y. Li, A. Sohani, J. M. Mabry and A. Tuteja, *Adv. Mater.*, 2012, 24, 3666.
54 J. Li, R. Kang, X. Tang, H. She, Y. Yang and F. Zha, *Nanoscale*, 2016, 8, 7638.
55 J. Li, Z. Zhao, D. Li, H. Tian, F. Zha, H. Feng and L. Guo, *Nanoscale* 2017, 9, 13610-13617.
56 J. Song, S. Huang, Y. Lu, X. Bu, J. E. Mates, A. Ghosh, R. Ganguly, C. J. Carmalt, I. P. Parkin, W. Xu and C. M. Megaridis, *ACS Appl. Mater. Inter*., 2014, 6, 19858.
57 P. Raturi, K. Yadav and J. P. Singh, *ACS Appl. Mater. Inter*., 2017, 9, 6007.
58 Z. Yu, F. F. Yun, Z. Gong, Q. Yao, S. Dou, K. Liu, L. Jiang and X. Wang, *J. Mater. Chem. A*, 2017, 5, 10821.
59 K. Yin, D Chu, X. Dong, C. Wang, J. Duan and J. He, *Nanoscale*, 2017, 9, 14229.
60 J. Gu, P. Xiao, P. Chen, L. Zhang, H. Wang, L. Dai, L. Song, Y. Huang, J. Zhang and T. Chen, *ACS Appl. Mater. Inter*., 2017, 9, 5968.
61 J. Fan, Y. Song, S. Wang, J. Meng, G. Yang, X. Guo, L. Feng and L. Jiang, *Adv. Funct. Mater*., 2015, 25, 5368.
62 H. Liu, J. Huang, Z. Chen, J. Chen, K. Zhang, S. S. Al-Deyab and Y. Lai, *Chem. Eng. J.*, 2017, 330, 26.
63 X. Hou, Y. Hu, A. Grinthal, M. Khan, J. Aizenberg, Nature, 2015519, 70.
64 X. Hou, *Adv. Mater.*, 2016, 28, 7049.
65 X. Tian, V. Jokinen, J. Li, J. Sainio and R. H. A. Ras, *Adv. Mater.*, 2016, 28, 10652